URS

EXPERIMENTAL INVESTIGATION OF RELATIVE RESPONSE OF ACCELEROGRAPH PAD, FREE FIELD AND STRUCTURAL FOUNDATIONS AT THE VIRGIL C. SUMMER NUCLEAR STATION

ADDENDUM

March 1983

prepared for

South Carolina Electric
and Gas Company
Columbia, South Carolina

prepared by

URS/John A. Blume & Associates, Engineers
2855 Telegraph Avenue
Berkeley, California 94705

CONTENTS

IX. ADDENDUM

OVERVIEW

This addendum presents the results of additional analyses of foundation/free field spectral modulus ratios, and appraises the data analysis and results given in the URS/Blume report to South Carolina Electric and Gas Company, Experimental Investigation of Relative Response of Accelerograph Pad, Free Field and Structural Foundations at the Virgil C. Summer Nuclear Station dated February 1983. As such it forms part of that report. Citations to text and figures therein are indicated by Roman numerals.

The additional analyses consist of developing spectral modulus ratios for horizontal components resolved according to the foundation axes, and axis-independent ratios formed from square root of the sum of the squares (SRSS) combination of the orthogonal components of motion in the foundation and free field. Spectral modulus ratios for signals rotated to coincide with the foundation axes do not show consistent differences for the two axes, as judged by comparing Test 3 and 4 results. Ratios for SRSS spectral moduli are nearly identical to those obtained in Chapter VI by treating the orthogonal component motions as independent trials of a generalized horizontal motion.

Additional documentation of the statistical dispersion in the spectral modulus ratios is also given. Geometric standard deviations of foundation/free field spectral modulus ratios, reflecting shot-to-shot and site-to-site variability are relatively independent of frequency and have a characteristic value close to 2 for Test 3. This result for Test 3 is not likely to seriously underestimate the overall dispersion of foundation/free-field motion, and is typical of seismologic data.

The cause of differences in detail between Test 3 and Test 4 results is investigated at further length. It is concluded as before that differences in detail are most reasonably explained as resulting from propagation effects unrelated to the actual ground-structure interaction phenomena under

investigation. The supplementary results and analysis of the nature of the recorded seismic signals lend support to the data analysis procedures used in Chapter VI.

SUPPLEMENTARY ANALYSIS

A. Background

In formulating the data analysis in Chapter VI, foundation/free field spectral modulus ratios for radial and transverse components were compared for Tests 3 and 4. It was observed that while the general levels were similar, the detail in these spectral ratios was not reproduced in the two tests, which differed by 40 degrees in azimuth. In particular, it was noted that peaks at 20 Hz in the radial component spectral modulus ratios for both the Auxiliary Building and Diesel Generator Building for Test 3 did not appear on either horizontal component for Test 4, suggesting that the detail in the spectral ratios was due to wave propagation effects that are unrelated to the actual interaction phenomena under investigation. Finally, it was concluded that there were no systematic differences, except in detail, between spectral modulus ratios for radial and transverse components, and on this basis the two components were treated as independent trials of a random process in a generalized horizontal direction. On the same basis, ratios for Tests 3 and 4 were combined by geometric averaging to form spectral modulus ratios for a generalized horizontal direction.

In this section, the detailed nature of the spectral modulus ratios is investigated further by forming ratios for horizontal components resolved according to the axes of the foundations, rather than in the radial and transverse directions employed for recording and for reporting results in Chapter VI. The use of polar coordinates in the experiment was motivated by one of the program objectives, namely to compare foundation and free field motions by wave type; ideally, SH or Love motion is polarized in the transverse direction while P-SV or Rayleigh motion is polarized in the radial-vertical plane.

The representation of the results given in Chapter VI as expressing ratios of translational "input" motion to translational free field motion is an idealization, and would be so even in the case of an ideally simple crustal structure. Motions recorded on the foundations are not strictly "input" motions in that they are influenced to some extent by modal responses of the ground-structure systems. For example, in the case of the Diesel Generator Building, the foundation is supported by caissons penetrating the saprolite to bedrock.

Modal effects could cause differences in motion for the two foundation axes and this provides the motivation for additional analyses to appraise the data reduction in Chapter VI. If observed, significant and consistent axial differences for the tests conducted would indicate the existence of real directional response that had been smoothed out.

Motions recorded by the seismometers on the foundations include a contribution due to rotation, which although unknown, is generally expected to be of the order of a few percent. For all three structures where the tests were recorded, the seismometers were situated near corners of the foundations and so are expected to register motions generally higher than elsewhere on the foundation. Therefore, results obtained from these data are subject to bias in the sense of overestimating the actual translational motion of the foundations.

It should be noted that the estimation of free-field and foundation motion corresponding to recorded accelerograph pad motion (Sections VI.D, E and F) was performed assuming single-input linear system behavior, with the magnitudes of the system transfer (or filter) functions equal to the spectral modulus ratios and the phase of the transfer functions equal to zero. Although not originally proposed, complete transfer functions as calculated from the measured pad or foundation and free-field motions were examined in an effort to determine the nature of the systems. A system coherence approaching a value of one over the full frequency band would have indicated single-input linear system behavior. Although the coherence had values near one in the frequency band up to 15 Hz, beyond this frequency the coherence was typically much lower, in which case the transfer function is not a good estimate of the relationship between input and output. Therefore, as proposed, the filters that were used had zero phase with

magnitudes equal to the spectral modulus ratios, which were described statistically. The lack of system coherence, particularly at the higher frequencies, is not surprising and may be largely due to phase incoherency of the signals, attributable to the effects of geologic heterogeneity.

B. Spectral Modulus Ratios of Horizontal Motions Resolved According to Foundation Axes

The angles between the foundation axes and the orientations of horizontal seismometers installed on the foundations for Tests 3 and 4 are listed in Table IX.B.1. For the spectral modulus ratios presented below, foundation signal and noise records were rotated by the angles specified in the table. Free field signal and noise records were likewise rotated by the same angles, so as to give the same relative contribution of radial and transverse components in the rotated foundation and free-field records. As noted in Section VI.C, free-field stations recording Tests 3 and 4 were deployed in arrays of apertur: 80 degrees and the directions of the new free-field axes vary over the same range. Foundation/free field spectral modulus ratios were computed for the rotated horizontal components in exactly the same manner as in Chapter VI.

Test 3 results for the Service Water Pumphouse are shown in Figures IX.B.1 and 2 for directions N 50.4 degrees E and N 39.6 degrees W, corresponding to the building axes. These results are very similar to those for the radial and transverse directions as given in Figures VI.C.14 and 15. A fairly prominent spectral ratio peak at 14 Hz is reduced in amplitude from about 0.6 for the transverse direction to about 0.4 for the NW building axis. Ratios for both radial and NE directions have similar peaks at 15 and 20 Hz. There are no usable data from Test 4 to evaluate the apparent differences in the spectral modulus ratios for the two foundation axes; the epicentral distance of the Service Water Pumphouse from Test 4 shots was about 500 ft (about 10 percent) greater than for the other foundations, and the horizontal component signals were rendered unusable because of high levels of ambient noise.

For this section, the significant results are those for the Auxiliary Building and Diesel Generator Building, where usable foundation signals were obtained for both Test 3 and Test 4, along with records at four and two equidistant

free-field sites respectively. The degree of resolution of real differences in foundation/free-field motion between one foundation axis and the other can be judged by comparing results for Tests 3 and 4.

Auxiliary Building foundation/free field spectral modulus ratios for records rotated to give N-S and E-W axes in the building are shown in Figures IX.B.3 and 4 for Test 3, and Figures IX.B.5 and 6 for Test 4. Comparing details for the N-S axis (Figures IX.B.3 and 5), a broad peak near 20 Hz for Test 3 is absent for Test 4, and a minimum at 23 Hz and a maximum at 30 Hz for Test 3 contrast with a maximum and a minimum, respectively, at these same frequencies for Test 4. Likewise, Test 3 and 4 results for the E-W axis are dissimilar in detail. Spectral modulus ratios for the same direction for the two tests (i.e., shot points 3 and 4) do not show more similarity in detail than do ratios for the same test for the two directions. These data do not indicate that spectral modulus ratios for the N-S and E-W directions are consistently different.

Results for the Diesel Generator Building for N-S and E-W axes are given in Figures IX.B.7 and 8 for Test 3, and Figures IX.B.9 and 10 for Test 4. For the N-S axis, results for Tests 3 and 4 bear resemblance in exhibiting a prominent peak, but not at the same frequency--20 Hz for test 3 versus 26 Hz for Test 4. For the E-W axis, the ratios bear resemblance in being smoother than most of the ratios reported herein, but the extrema of these ratios are respectively a maximum and a minimum at 10 Hz for Tests 3 and 4. Again the data do not indicate that ratios for the N-S and E-W directions are consistently different.

C. Ratios of SRSS Spectral Moduli

The results reported in this section were computed by taking the square root of the sum of the squares (SRSS) of the spectral moduli of the orthogonal components and then forming foundation/free field ratios. The motivation for this analysis was to form ratios of axis-independent quantities. The SRSS function is the square root of the horizontal power spectral density.

Foundation/free field SRSS spectral modulus ratios for the Service Water Pumphouse (Test 3), Auxiliary Building (Tests 3 and 4), and Diesel Generator

Building (Tests 3 and 4) are shown in figures IX.C.1, 2, 3, 4 and 5. These results are nearly identical to ratios given in Chapter VI for combined horizontal components (see Figures VI.C.16, 20, 24, 28 and 32), wherein radial and transverse motions are treated as independent trials of a random process in a generalized horizontal direction. Note that the SRSS ratios are less variable between Tests 3 and 4 than are the single-component ratios.

D. Estimation of Dispersion in Spectral Modulus Ratios

As discussed in Section V.C and as illustrated in Figures V.C.7, 8 and 9, statistics of foundation/free field spectral modulus ratios for a data set with a multiplicity of free-field receivers and of shots at a given location can be computed to exhibit the variability from shot to shot, from site to site, or combined shot-to-shot and site-to-site. For Test 3 there are sufficient equidistant free-field sites for calculating statistics of site-to-site dispersion. In the case of all foundation/free field ratios reported for Test 3, the spectral modulus in the denominator is the average taken over all free-field sites, and standard deviations shown in the plots display the shot-to-shot variability for the test sequence. These plots do not display the overall dispersion, including that between free field sites, of foundation/free field ratios. Statistics of foundation/free field ratios for Test 4 were calculated from the individual pairs of foundation and free field records, i.e. without forming average free-field spectral moduli for each shot. The standard deviations in the plots therefore display the variability from shot to shot and between the two free-field sites. In summary, standard deviations shown in the Chapter VI plots for Test 3 display only the shot-to-shot variability, while for Test 4 the overall dispersion of the data set is displayed.

The purpose of this section is to present Test 3 foundation/free field results that display the overall standard deviations due to shot-to-shot and site-to-site dispersion. These are given in Figures IX.D.1, 2 and 3 for the Service Water Pumphouse, Auxiliary Building, and Diesel Generator Building respectively. For all three cases the geometric standard deviation is relatively independent of frequency and has a characteristic value of 2, which is quite typical for seismologic data. Results for Test 4 are given in Figures VI.C.24 and VI.C.32 for the Auxiliary Building and Diesel Generator Building

respectively. These show smaller standard deviations than for Test 3, and this is attributable to the fact that there were just two equidistant free-field stations for Test 4.

The standard deviations obtained for Test 3 serve only as an approximation of the overall variability of foundation/free field motion, which cannot be established rigorously from these data. In view of the dissimilarity at some frequencies of Test 3 and Test 4 spectral modulus ratios, the Auxiliary Building/free field results for Test 1 shown in Figure VI.C.48 are informative in providing data from a third shotpoint location. The results for Tests 1, 3 and 4 are similar in terms of average ratio (about 0.5 or less) for horizontal components in the band 5-35 Hz, with an overall tendency of the ratio to increase with frequency above 10 Hz. This comparison suggests that the standard deviations obtained for Test 3 are not likely to seriously underestimate the overall variability of foundation/free field motion.

Final results used for computing foundation response spectra in Chapter VI were obtained, in the case of the Auxiliary Building and Diesel Generator Building, by computing the geometric average of the means for the two tests (Figures VI.C.20 and 24, and figures VI.C.28 and 32 respectively). No attempt was made to compute the statistics of these results because of the unreliability of the standard deviations for the Test 4 data.

The averaging procedure used to derive the final horizontal motion ratios in Chapter VI assumes that the data of Tests 3 and 4 sample the same parent population of foundation/free field spectral modulus ratios. The same assumption underlies the averaging of spectral modulus ratios for the shot sequence of each test, using all free field data at comparable distance. The validity of these assumptions is not demonstrable from the ratios themselves, and is instead appraised below, using as a basis seismologic information presented in Chapter IV on the nature of the seismic signals and their variability.

DISCUSSION

The supplementary analyses reported above were prepared with the aim to further investigate the nature of the detail exhibited in the foundation/free field spectral modulus ratios given in Chapter VI. Of particular importance was the question as to whether the treatment of the horizontal components as independent trials of generalized horizontal motion was appropriate, in view of the potential that the recorded foundation motions, influenced to some extent by modal responses of the ground-structure systems, might differ significantly and consistently in the orthogonal axes of the buildings. However, results of the supplementary analyses do not show consistent differences between orthogonal building axes. Such differences as may exist are obscured by variations due to phenomena that are not reproducible for Tests 3 and 4.

The assessment of features in the spectral modulus ratios that are not reproducible in Tests 3 and 4 is important to the overall appraisal of the foundation/free field results. The factors that are germane to the actual interaction effects under consideration are the differences in distance and azimuth of the test locations. Because the difference in distance is small (3700 ft for Test 3 vs. 4300 ft for Test 4), differences in body-wave angles of incidence would also be small, as the apparent velocities do not change significantly over this range (see Figure IV.B.1). Secondly, while foundation motion may be expected to depend on the azimuth of incoming wave fronts, this effect is not large enough to account for the differences in spectral modulus ratios for Tests 3 and 4. The remaining factors to be considered are radial asymmetry of the wave field generated by the explosions and complex propagation effects in the near vicinity of the receivers, producing effects in the spectral ratios that are unrelated to the actual interaction effects under investigation. The results given in Chapter VI were obtained on the premise that these extraneous propagation effects account for the differences in spectral modulus ratios for Tests 3 and 4, and for the differences in detail between ratios for orthogonal components.

This premise is supported by the analysis given in Chapter VI of the data for the USGS accelerograph pad and free field array. Because of the relative simplicity of the pad-soil system, there is no reason to expect widely

divergent soil-structure interaction per se for the two pad axes or for incoming wave fronts of different azimuths, and yet widely divergent spectral modulus ratios were obtained. This can be ascertained by inspecting accelerograph pad/free field spectral ratios for Test 4 (Figures VI.B.5 and 6) and Test 5 (Figures VI.B.8 and 9) for the same free field station (P4). These variations are no less substantial than appear in the VCSNS foundaton/free field spectral modlus ratios, and so it is reasonable to infer that in both cases propagation effects unrelated to foundation/free field response are primarily reponsible for the variability of the ratios.

The complexity of the seismic signatures, evidenced by substantial site-to-site variability over distances of tens of feet for the dam abutment array, is also indicated by the complex particle motions presented in Chapter IV. As shown in Chapter IV, particle motions for the 16 October 1979 earthquake as recorded by the USGS accelerograph on the dam abutment exhibit a degree of complexity comparable to particle motions for the explosion-generated waves. It is inferred that incoherence due to complex wave propagation effects, particularly in the near vicinity of receiver sites, is a general characteristic of seismic signals in the Monticello region, whether generated by earthquakes or explosions.

In summary, features in the spectral modulus ratios that are not reproducible in Tests 3 and 4 are readily explained in terms of extraneous propagation effects as evidenced by comparing data from free field sites. Alternative explanations are much less plausible. Results presented in Section IX.B do not indicate that spectral modulus ratios for the axial N-S and E-W directions are consistently different, either for the Auxiliary Building or for the Diesel Generator building. The same conclusion was reached in Chapter VI with respect to the radial and transverse directions. These observatons are consistent with the treatment of orthogonal horizontal components as independent trials of a random process in a generalized horizontal direction (as is conventional in the analysis of strong motion data). The results given in Chapter VI, which were used in developing foundation response spectra, were obtained by treating radial and transverse components in this manner. Nearly identical results were obtained in Section IX.C by taking the square root of

the sum of the squares of the horizontal component spectral moduli before forming the ratios, and this properly preserves horizontal power spectral density.

The results given in Chapter VI provide reasonable expectations of differences between foundation and free-field motion in that the variability of the spectral modulus ratios is most reasonably explained by complex propagation effects. The foundation/free field results are subject to bias (expected to be minor) in the sense of overestimating the actual translational motion, because the seismometers were placed near the corners of the foundations, where the recorded motions will include rotational contributions. The geometric standard deviations of the spectral modulus ratios for Test 3 have a characteristic value close to 2, which is typical of seismologic data. The Test 3 standard deviations are unlikely to seriously underestimate the overall dispersion of foundation/free field motion. However, it is evident that most of this dispersion is due to effects unrelated to the actual foundation/free field phenomena under investigation.

TABLE IX.B.1

ORIENTATION OF FOUNDATION SEISMOMETERS

RELATIVE TO BUILDING AXES

Structure	Azimuth of reference axis (degrees)	Radial azimuth-reference axis azimuth (degrees)	
		Test 3	**Test 4**
Auxiliary Building	0	20.5	60.8
Diesel Generator Building	0	25.4	63.7
Service Water Pumphouse	50.4	-18.3	16.0

URS/Blume

TABLE IX.B.2

LOG OF NEW SPECTRAL MODULUS CALCULATIONS

Run #	Test	Shot #s	Receivers X/Y	Component	Code Revision #	Comments *
279	3	2,3,6,7,8,	GS/F1 GS/F3 GS/F6 GS/FR	NORTH	5	North component is rotated 115 degrees counterclockwise from transverse component. 5 groups, 4 pairs per group.
280	3	2,3,6,7,8	GS/F1 GS/F3 GS/F6 GS/FR	WEST	5	West component is rotated 115 degrees counterclockwise from transverse component. 5 groups, 4 pairs per group.
281	3	2,3,6,7,8	AB/F1 AB/F3 AB/F6 AB/FR	NORTH	5	North component is rotated 111 degrees counterclockwise from transverse component. 5 groups, 4 pairs per group.
282	3	2,3,6,7,8	AB/F1 AB/F3 AB/F6 AB/FR	WEST	5	West component is rotated 111 degrees counterclockwise from transverse component. 5 groups, 4 pairs per group.
283	4	3,4,6 7,9	AB/P3 AB/F5 AB/F5	NORTH	5	North component is rotated 151 degrees counterclockwise from transverse component. No groups.
284	4	3,4,6 7,9	AB/P3 AB/F5 AB/F5	WEST	5	West component is rotated 151 degrees clockwise from transverse component. No groups.
285	3	2,3,6,7,8	GS/F1 GS/F3 GS/F6 GS/FR	SRSS	5	SRSS of the two horizontal components R and T. 5 groups, 4 pairs per group.
286	4	3,4,6, 7,9	AB/P3 AB/F5 AB/F5	SRSS	5	SRSS of the two horizontal components R and T. No groups.

URS/Blume

TABLE IX.B.2 (Continued)

Run #	Test	Shot #s	Receivers X/Y	Component	Code Revision #	Comments *
287	3	2,3,6,7,8	AB/F1 AB/F3 AB/F6 AB/FR	SRSS	5	SRSS of the two horizontal components R and T. 5 groups, 4 pairs per group.
288	4	3,4,6 7,9	GS/P3 GS/F5 GS/F5	SRSS	5	SRSS of the two horizontal components R and T. No groups.
289	4	3,4,6 7,9	GS/P3 GS/F5 GS/F5	NORTH	5	North component is rotated 154 degrees counterclockwise from transverse component. No groups.
290	4	3,4,6 7,9	GS/P3 GS/F5 GS/F5	WEST	5	West component is rotated 154 degrees counterclockwise from transverse component. No groups.
291	3	2,3,6,7,8	WP/F1 WP/F3 WP/F6 WP/FR	NE	5	NE component is rotated 72 degrees counterclockwise. 5 groups, 4 pairs per group.
292	3	2,3,6,7,8	WP/F1 WP/F3 WP/F6 WP/FR	NW	5	NW component is rotated 72 degrees counterclockwise from transverse component. 5 groups, 4 pairs per group.
297	3	2,3,6,7,8	AB/F1 AB/F3 AB/f6 AB/FR	R+T	5	No groups
298	3	2,3,6,7,8	GS/F1 GS/F3 GS/F6 GS/FR	R+T	5	No groups
299	3	2,3,6,7,8	WP/F1 WP/F3 WP/F6 WP/FR	R+T	5	No groups

* Whole record (512 points) .6-point Bartlett smoothing window. Power spectral noise was subtracted.

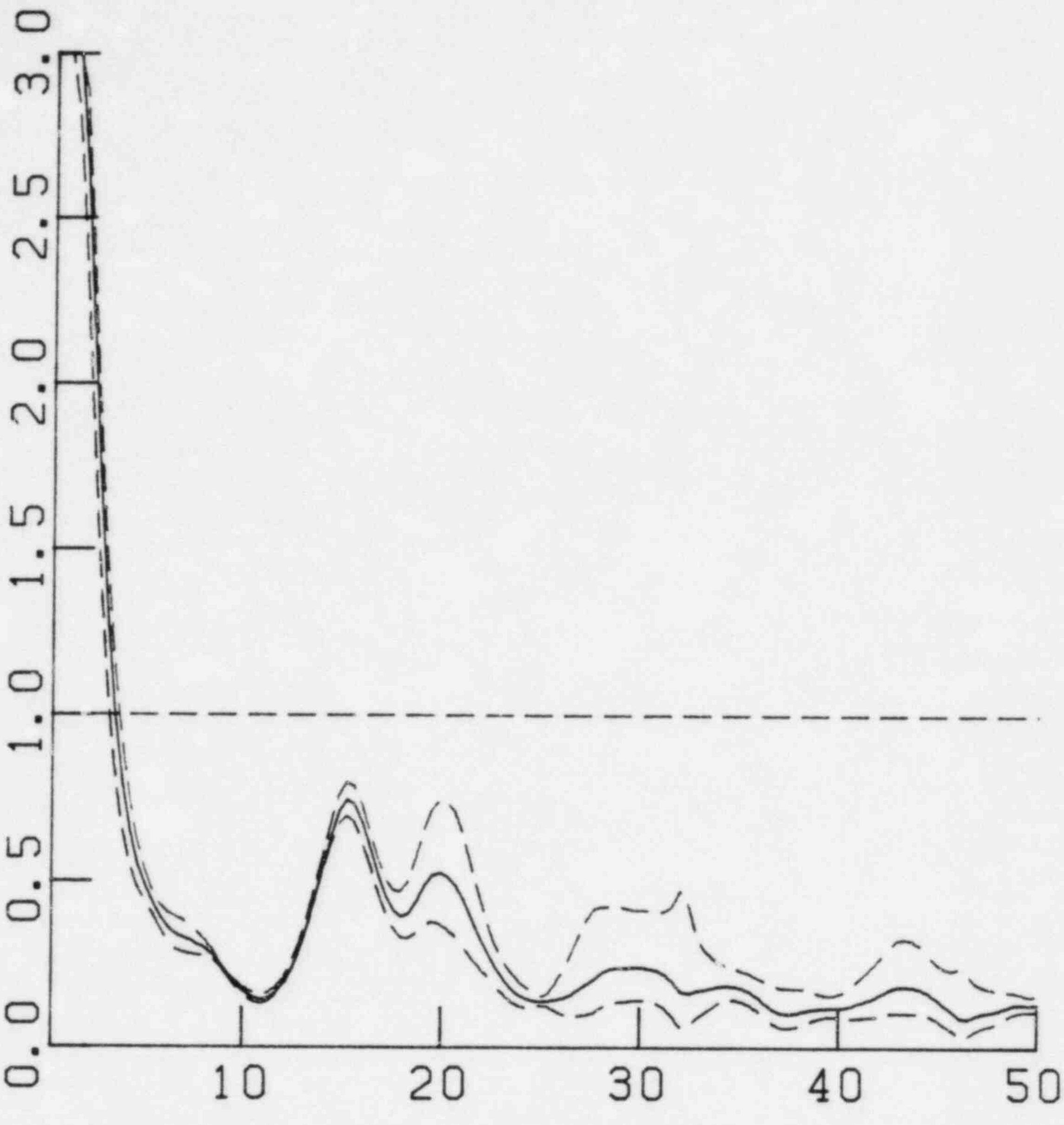

TEST 3, WP/FF, SHOTS 2,3,6,7,8, NE
RATIOS FROM MODULI IN GROUPS OF 4 ,5 GROUPS
RUN NO 291
POWER SPECTRAL NOISE SUBTRACTED

Figure IX.B.1 Service Water Pumphouse foundation/free field spectral modulus ratio of Test 3 seismograms rotated so as to coincide in the building with its northeast axis.

URS/Blume

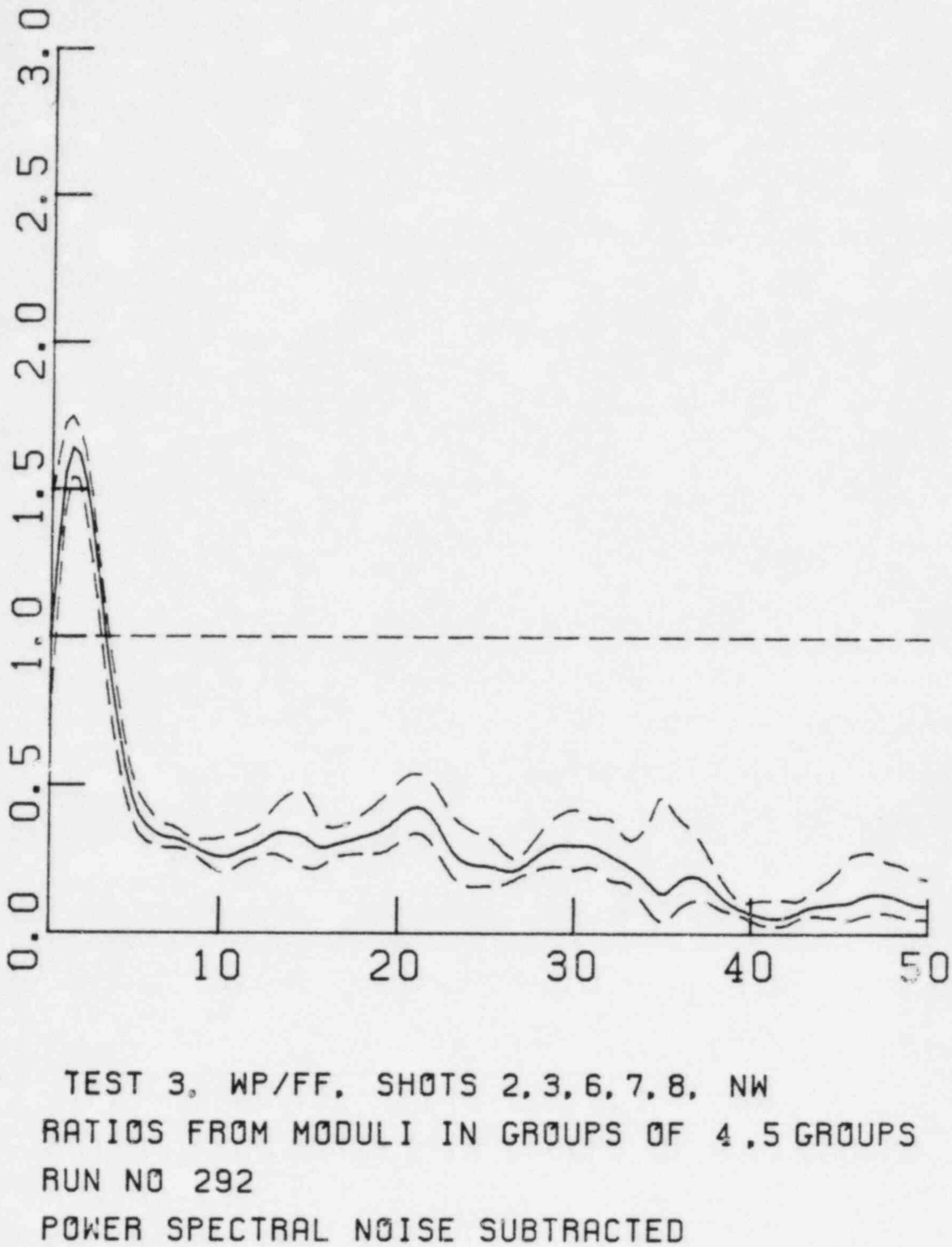

TEST 3, WP/FF, SHOTS 2,3,6,7,8, NW
RATIOS FROM MODULI IN GROUPS OF 4 ,5 GROUPS
RUN NO 292
POWER SPECTRAL NOISE SUBTRACTED

Figure IX.B.2 Service Water Pumphouse foundation/free field spectral modulus ratio of Test 3 seismograms rotated so as to coincide in the building with its northwest axis.

URS/Blume

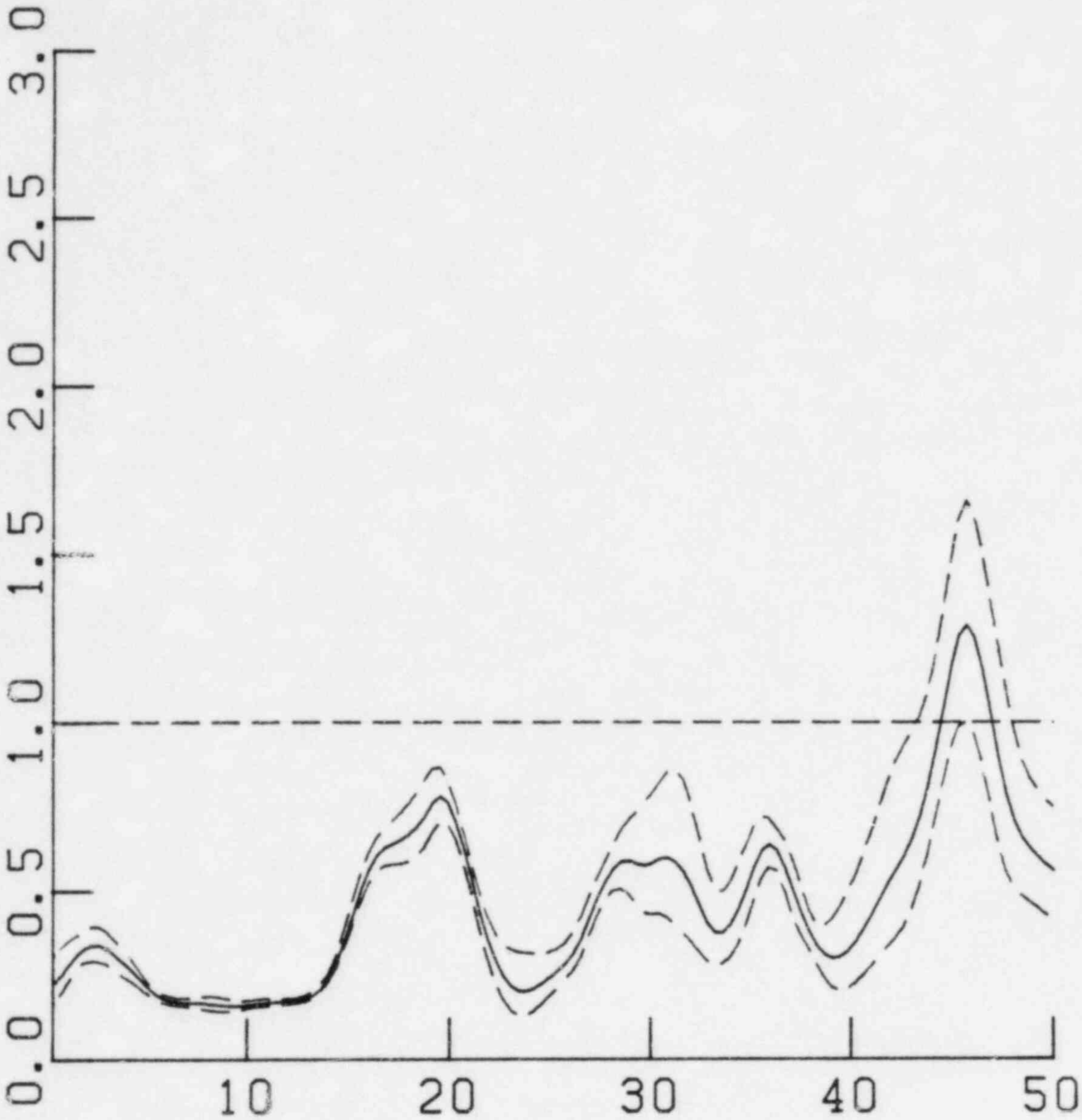

Figure IX.B.3 Auxiliary Building foundation/free field spectral modulus ratio of Test 3 seismograms rotated so as to coincide in the building with its north-south axis.

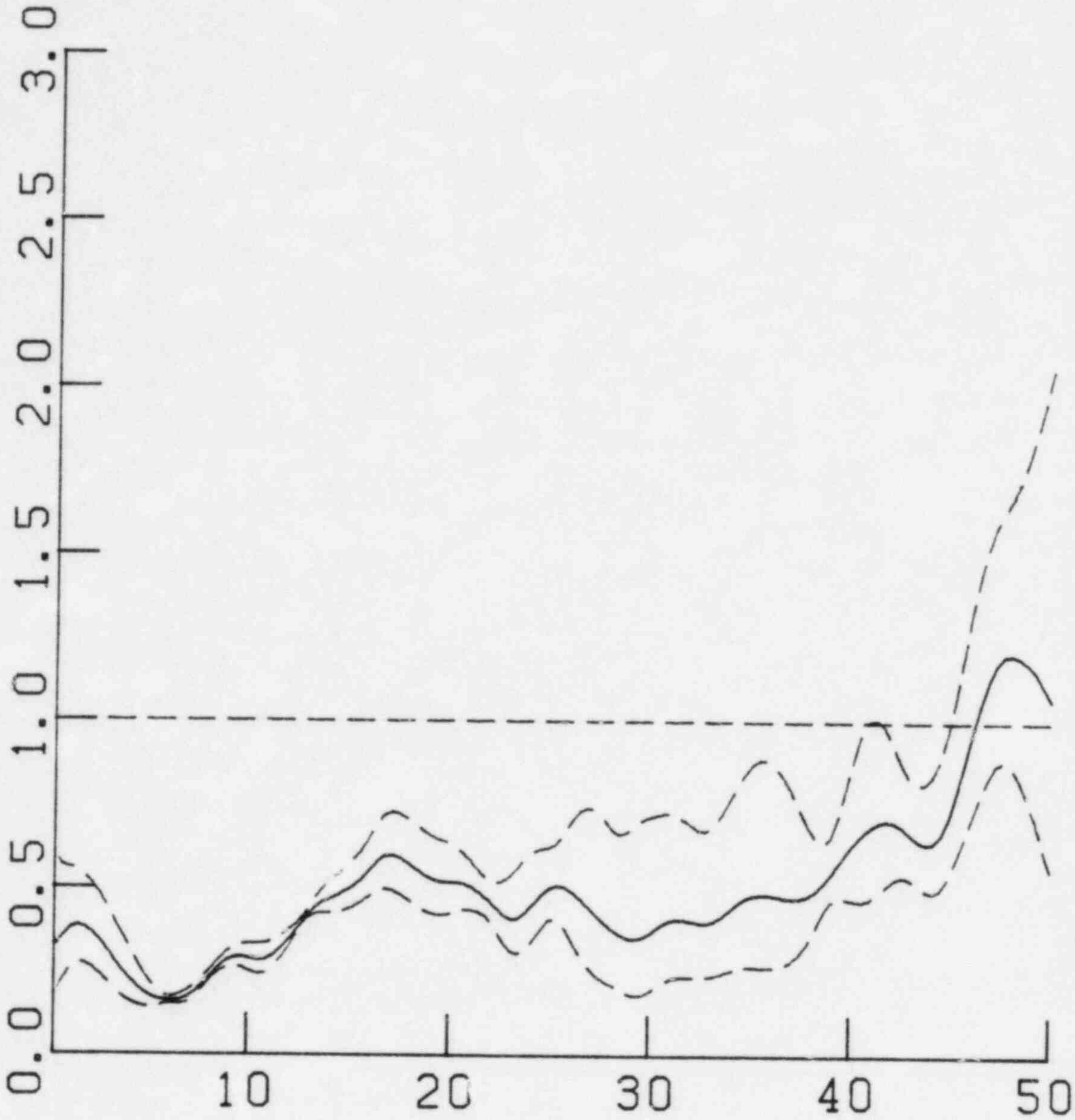

Figure IX.B.4 Auxiliary Building foundation/free field spectral modulus ratio of Test 3 seismograms rotated so as to coincide in the building with its east-west axis.

URS/Blume

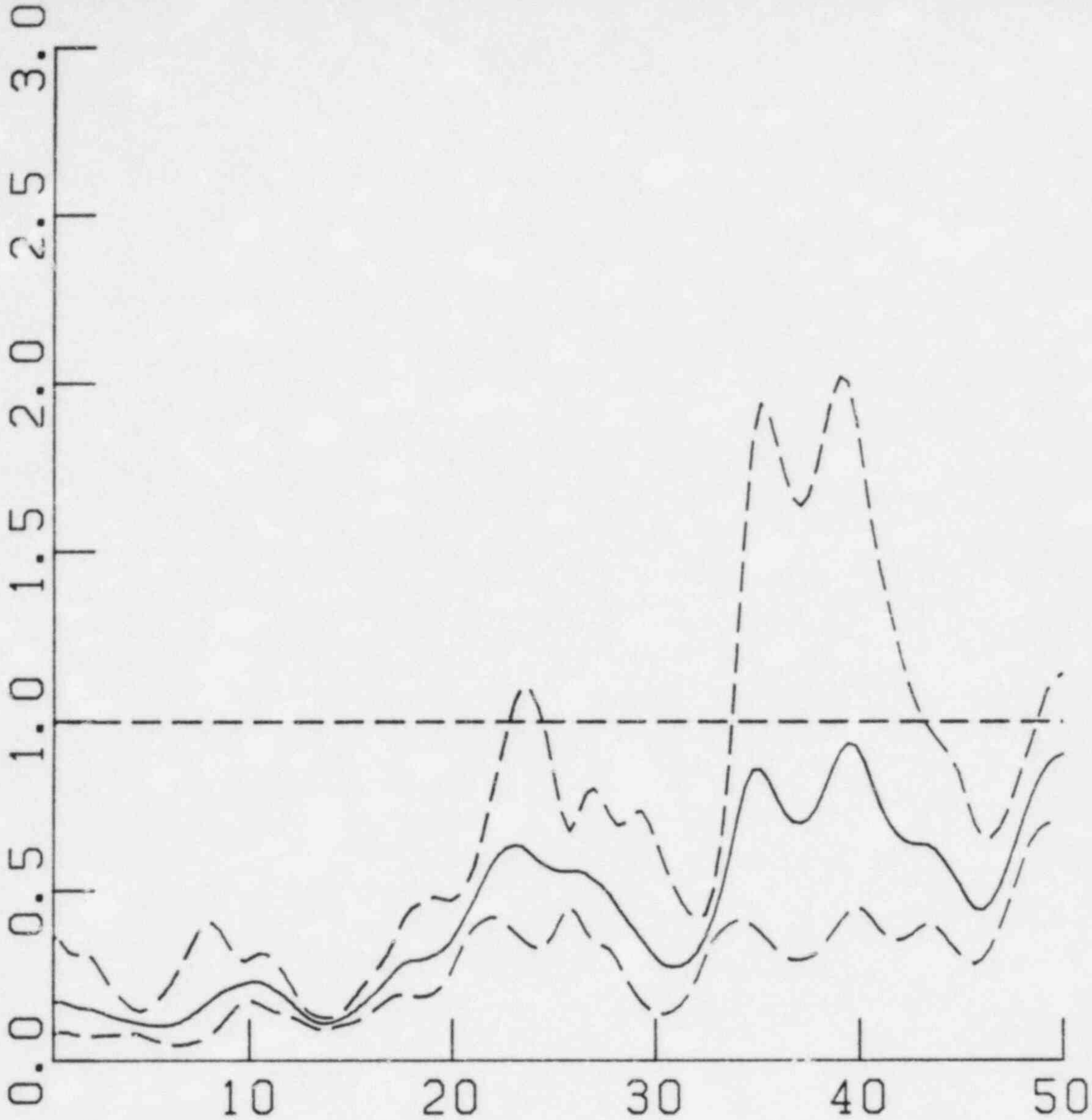

TEST 4 SHOTS 3, 4, 6, 7, 9 AB/<P3, F5> NORTH
RATIOS FROM MODULI INDIVIDUALLY
RUN NO 283
POWER SPECTRAL NOISE SUBTRACTED

Figure IX.B.5 Auxiliary Building foundation/free field spectral modulus ratio of Test 4 seismograms rotated so as to coincide in the building with its north-south axis.

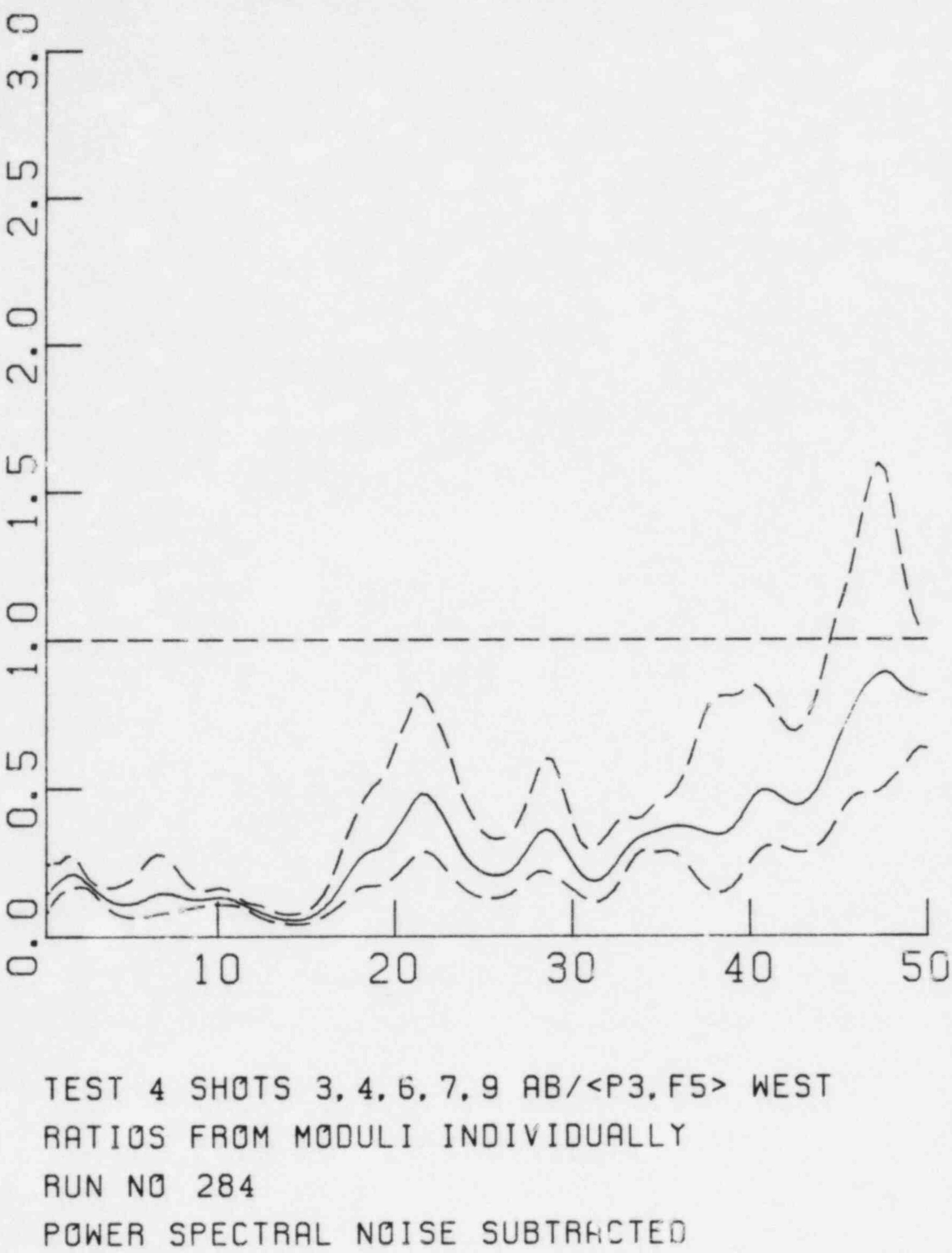

Figure IX.B.6 Auxiliary Building foundation/free field spectral modulus ratio of Test 4 seismograms rotated so as to coincide in the building with its east-west axis.

URS/Blume

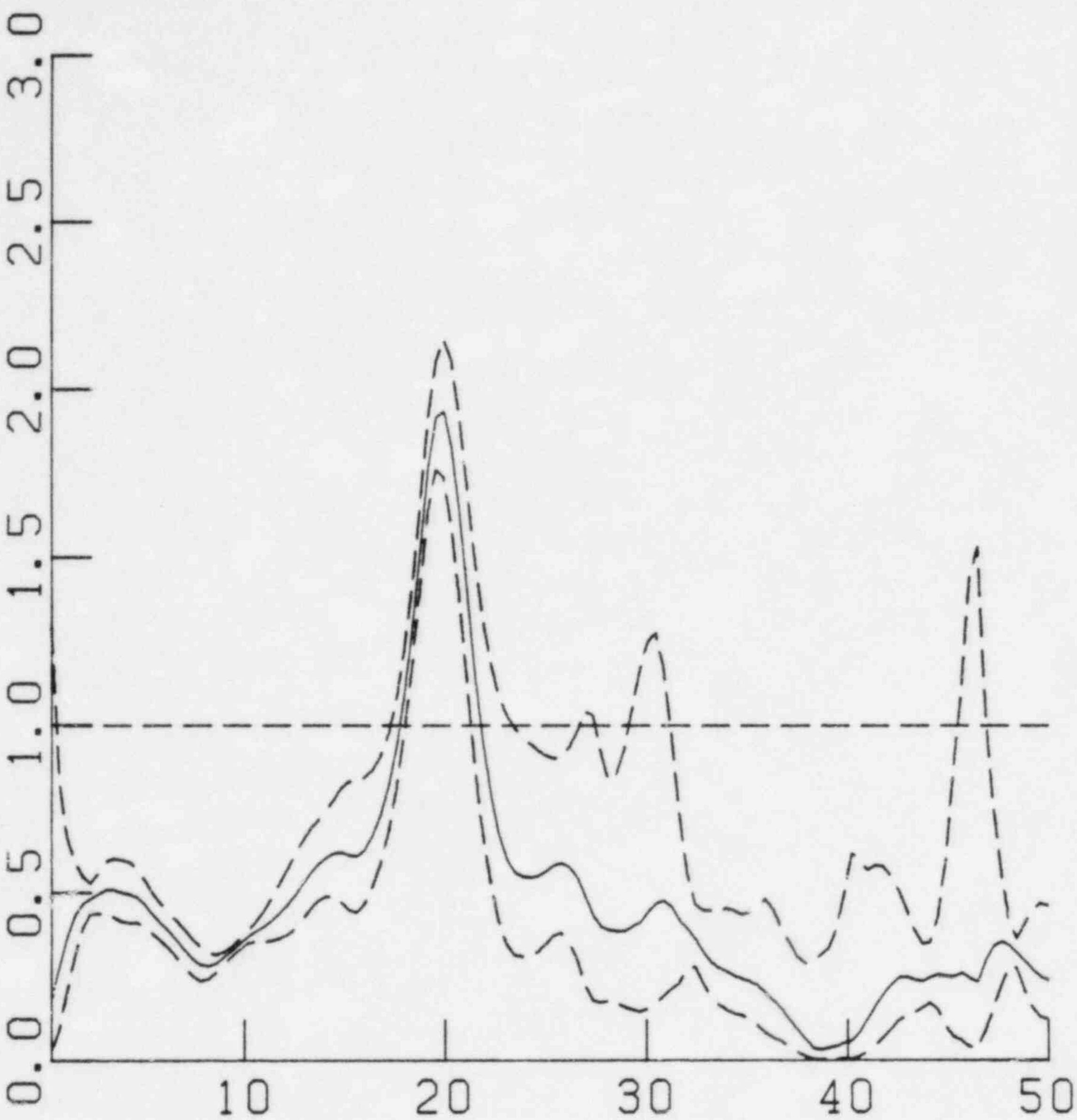

TEST 3, GS/FF, SHØTS 2,3,6,7,8, NØRTH
RATIØS FRØM MØDULI IN GRØUPS ØF 4,5 GRØUPS
RUN NØ 279
PØWER SPECTRAL NØISE SUBTRACTED

Figure IX.B.7 Diesel Generator Building foundation/free field spectral modulus ratio of Test 3 seismograms rotated so as to coincide in the building with its north-south axis.

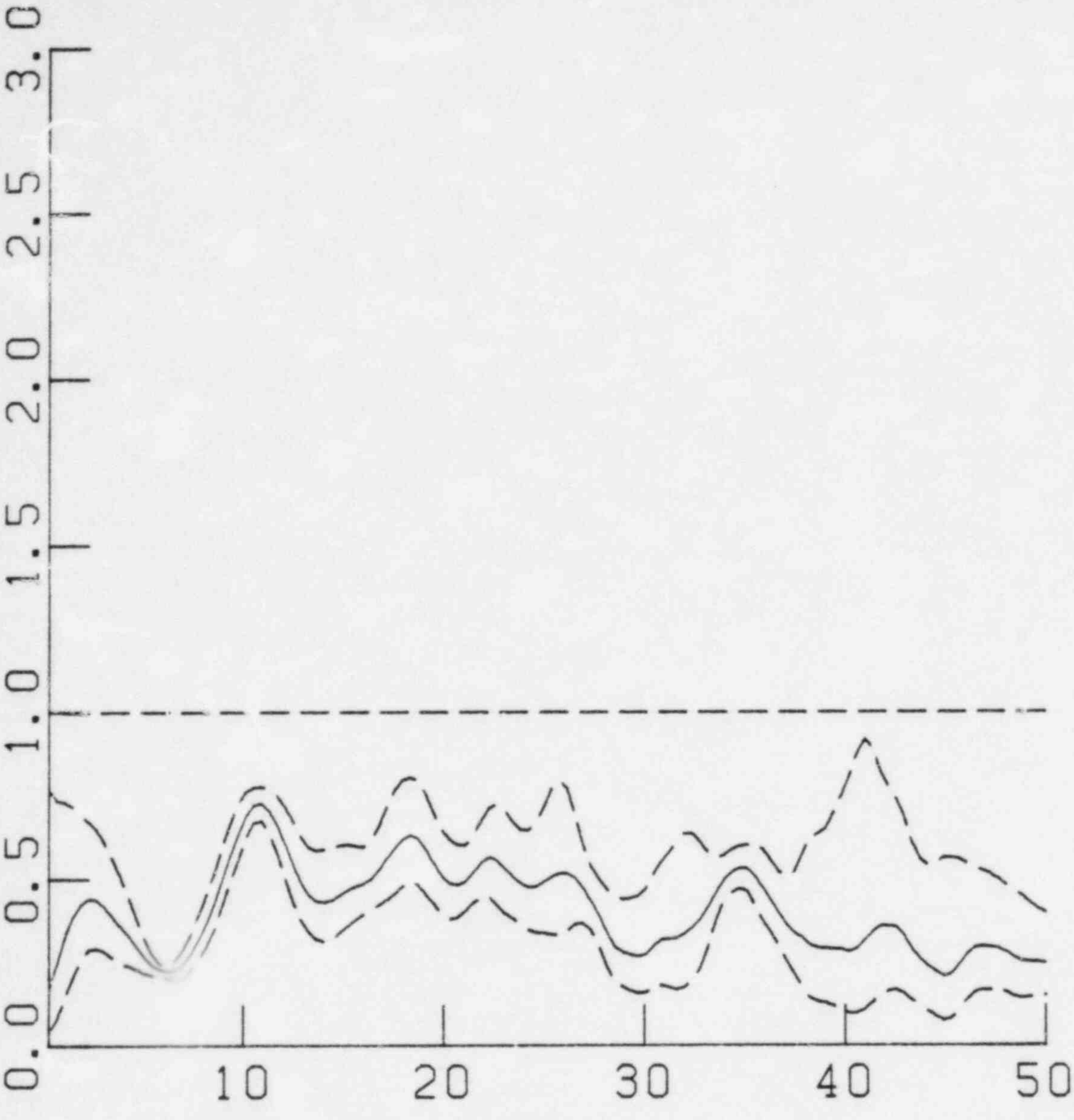

TEST 3, GS/FF, SHOTS 2,3,6,7,8, WEST
RATIOS FROM MODULI IN GROUPS OF 4 ,5 GROUPS
RUN NO 280
POWER SPECTRAL NOISE SUBTRACTED

Figure IX.B.8 Diesel Generator Building foundation/free field spectral modulus ratio of Test 3 seismograms rotated so as to coincide in the building with its east-west axis.

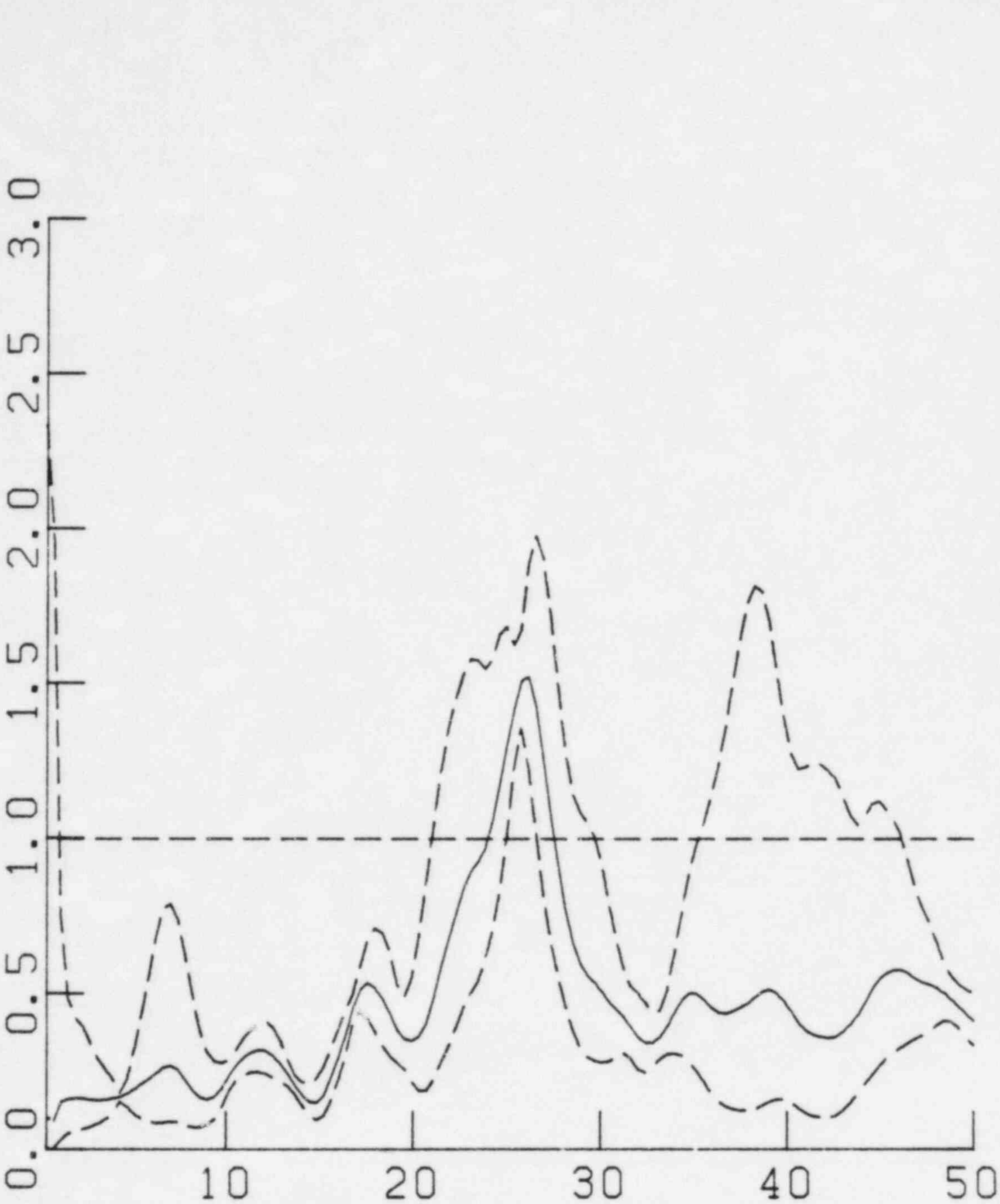

TEST 4 SHOTS:3 GS/<P3,F5> & 7,9 GS/F5 NORTH
RATIOS FROM MODULI INDIVIDUALLY
RUN NO 289
POWER SPECTRAL NOISE SUBTRACTED

Figure IX.B.9 Diesel Generator Building foundation/free field spectral modulus ratio of Test 4 seismograms rotated so as to coincide in the building with its north-south axis.

URS/Blume

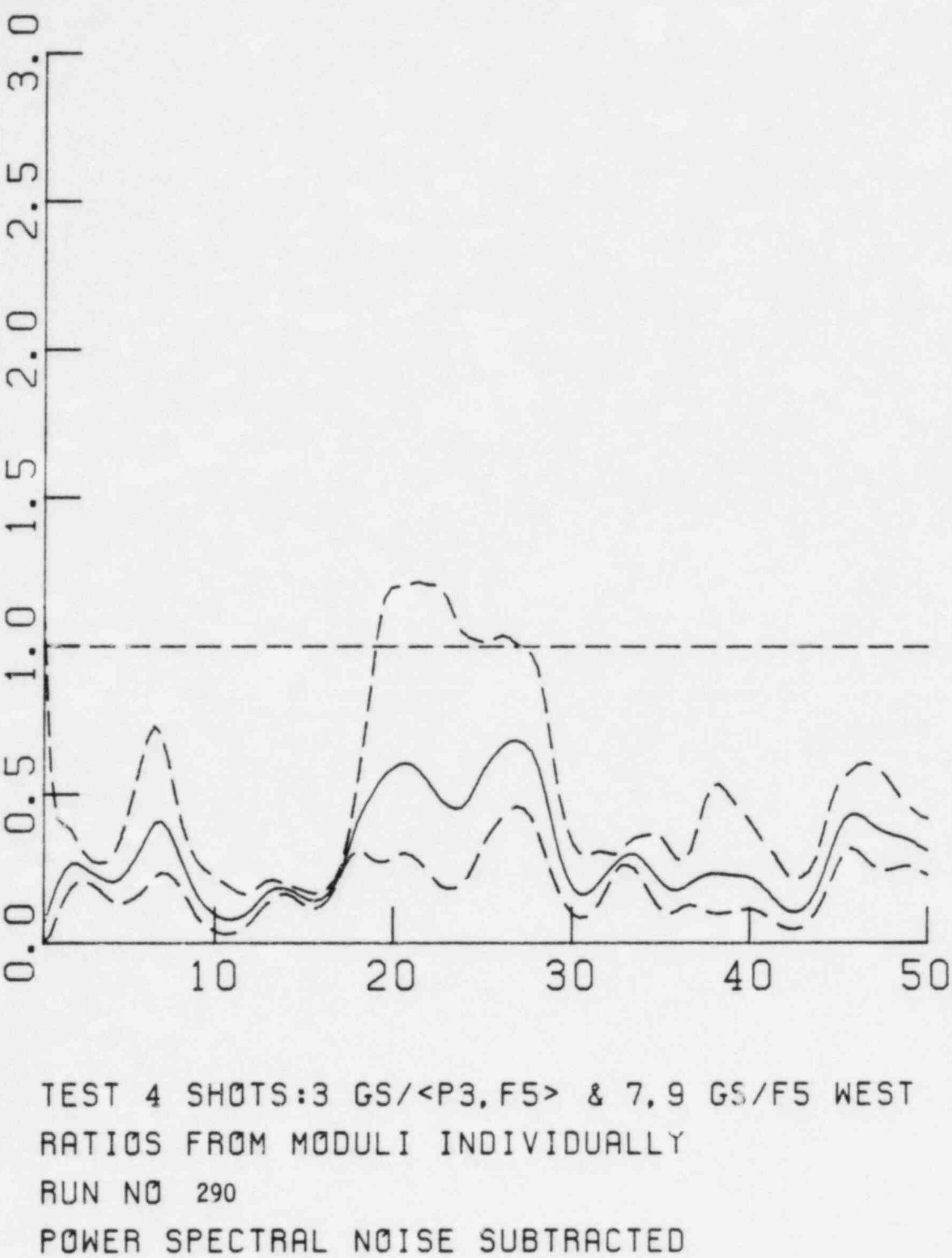

Figure IX.B.10 Diesel Generator Building foundation/free field spectral modulus ratio of Test 3 seismograms rotated so as to coincide in the building with its east-west axis.

URS/Blume

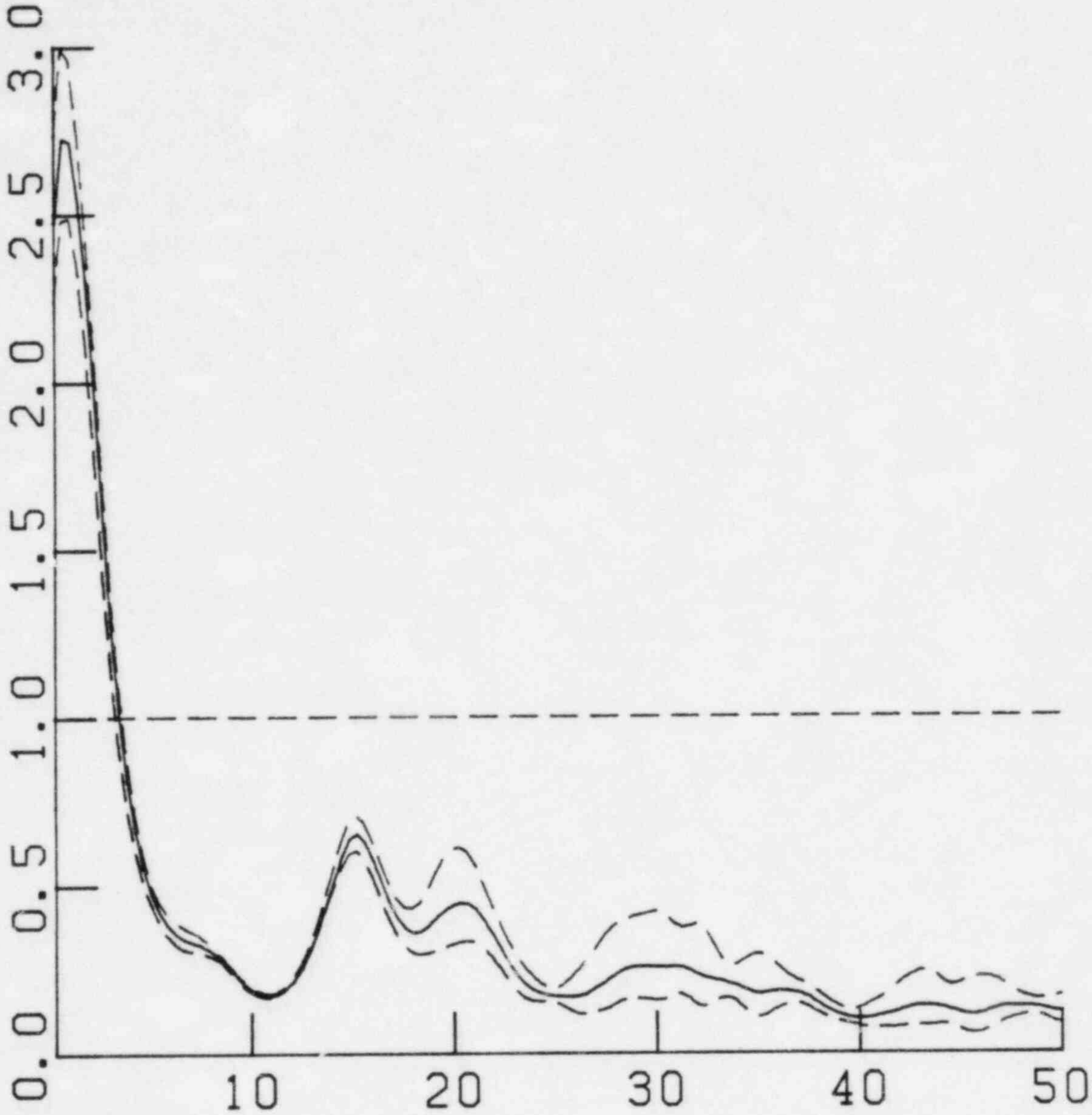

TEST 3, WP/FF, SHOTS 2, 3, 6, 7, 8, SRSS
RATIOS FROM MODULI IN GROUPS OF 4 .5 GROUPS
RUN NO 293
POWER SPECTRAL NOISE SUBTRACTED

Figure IX.C.1 Service Water Pumphouse foundation/free field SRSS spectral modulus ratio for Test 3. Compare with results in Figure VI.C.16, used in generating foundation response spectra.

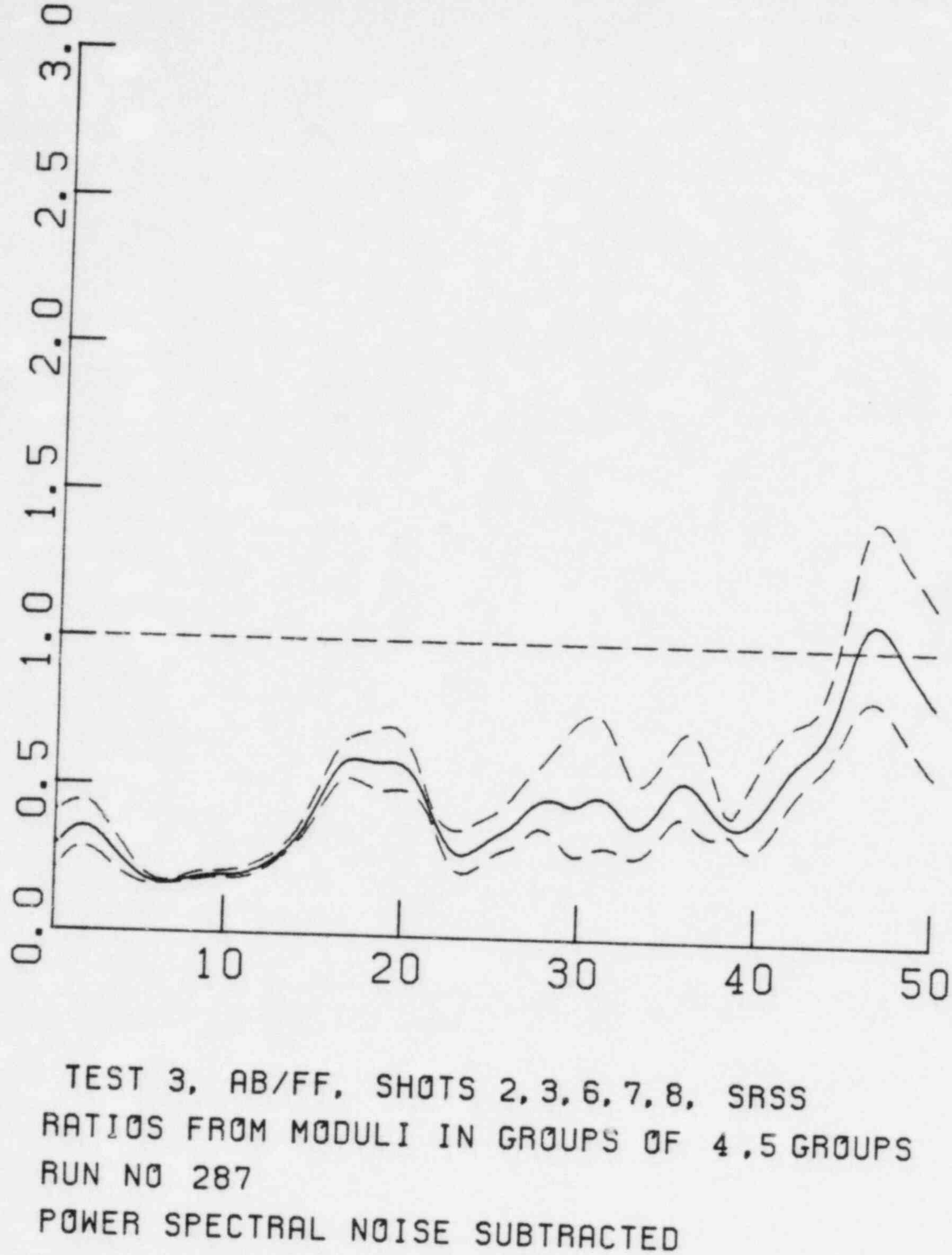

Figure IX.C.2 Auxiliary Building foundation/free field SRSS spectral modulus ratio for Test 3. Compare with results in Figure VI.C.20.

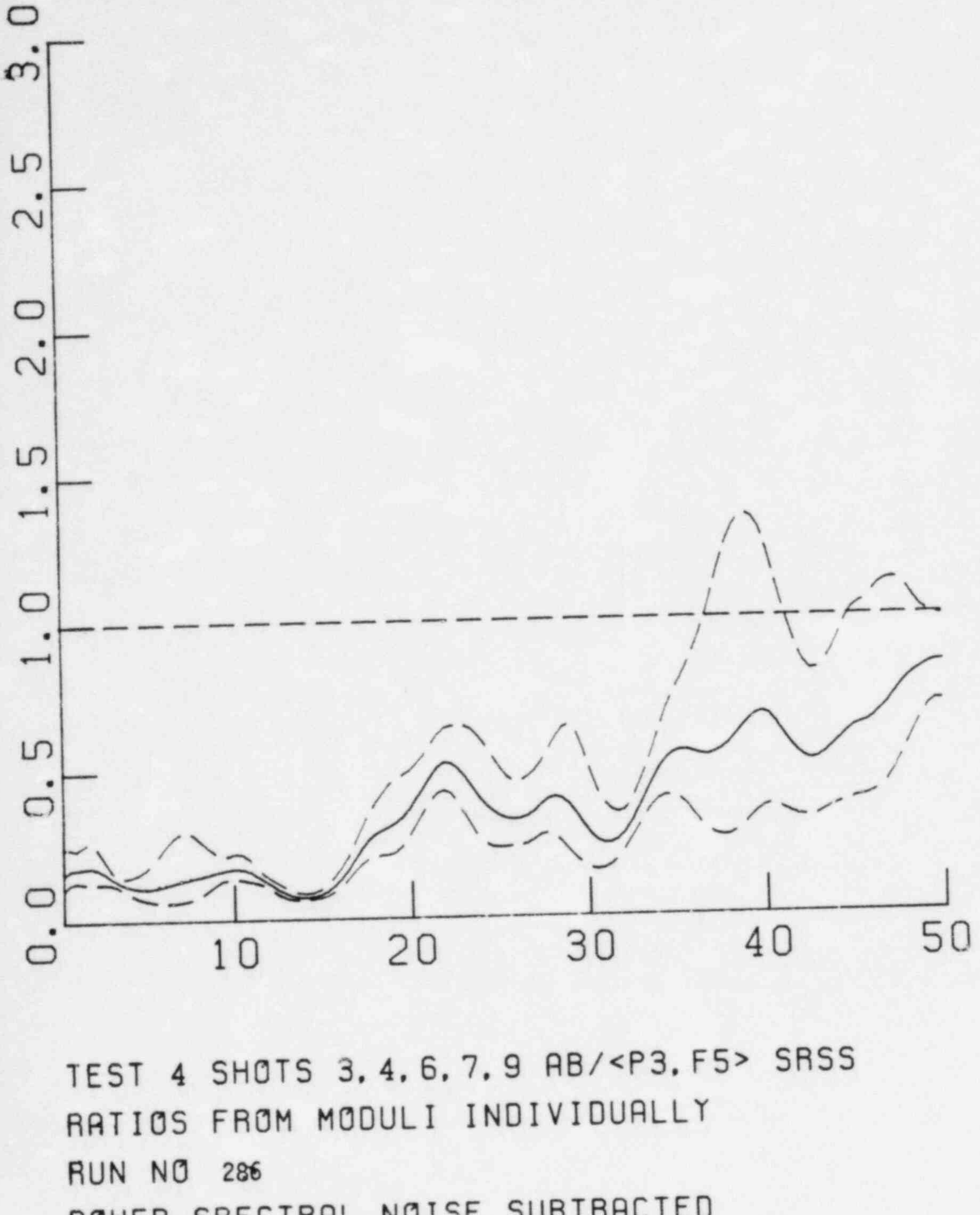

TEST 4 SHOTS 3, 4, 6, 7, 9 AB/<P3, F5> SRSS

RATIOS FROM MODULI INDIVIDUALLY

RUN NO 286

POWER SPECTRAL NOISE SUBTRACTED

Figure IX.C.3 Auxiliary Building foundation/free field SRSS spectral modulus ratio for Test 4. Compare with results in Figure VI.C.24.

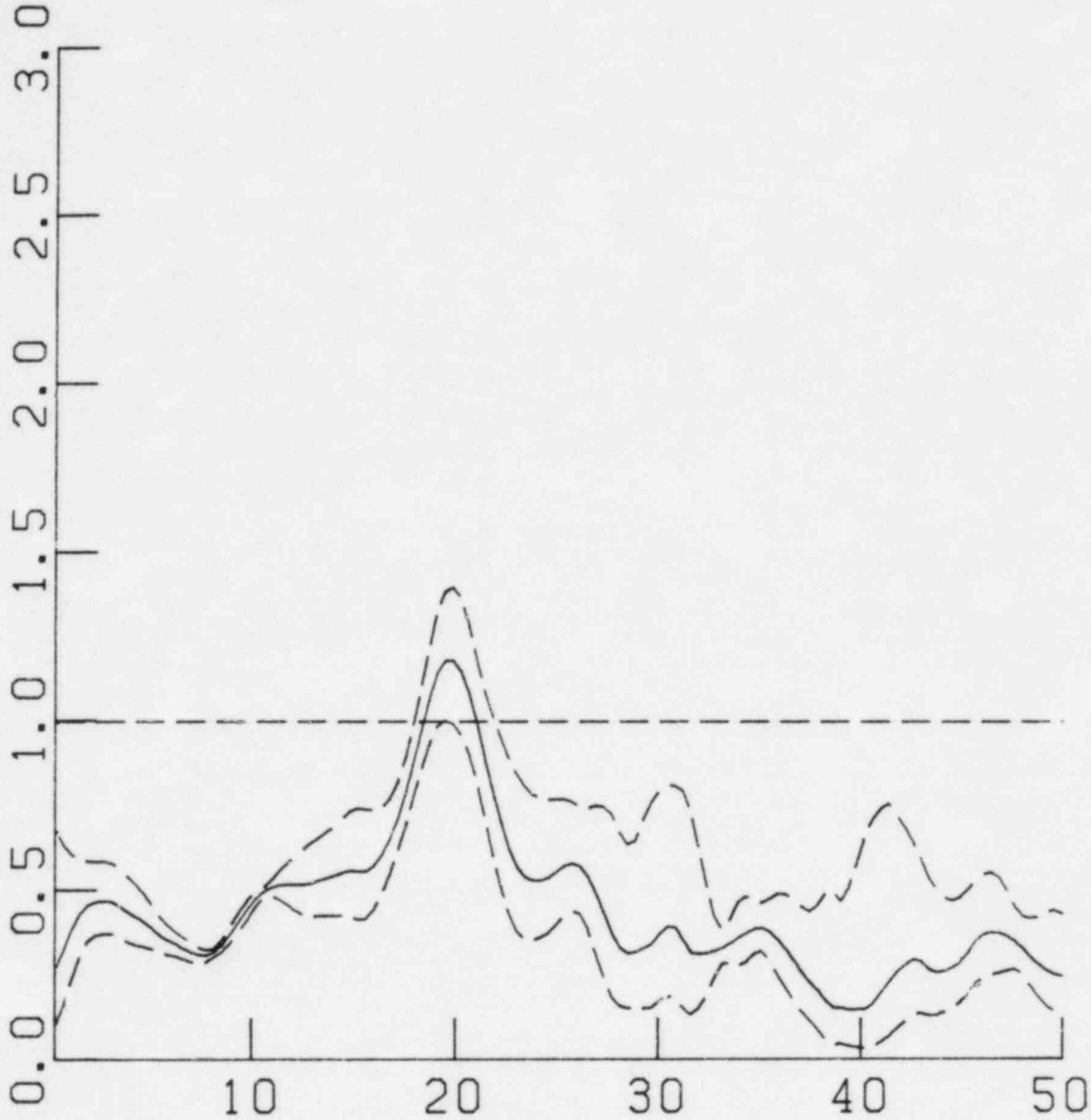

TEST 3, GS/FF, SHOTS 2,3,6,7,8, SRSS
RATIOS FROM MODULI IN GROUPS OF 4.5 GROUPS
RUN NO 285
POWER SPECTRAL NOISE SUBTRACTED

Figure IX.C.4 Disel Generator Building foundation/free field SRSS spectral modulus ratio for Test 3. Compare with results in Figure VI.C.28.

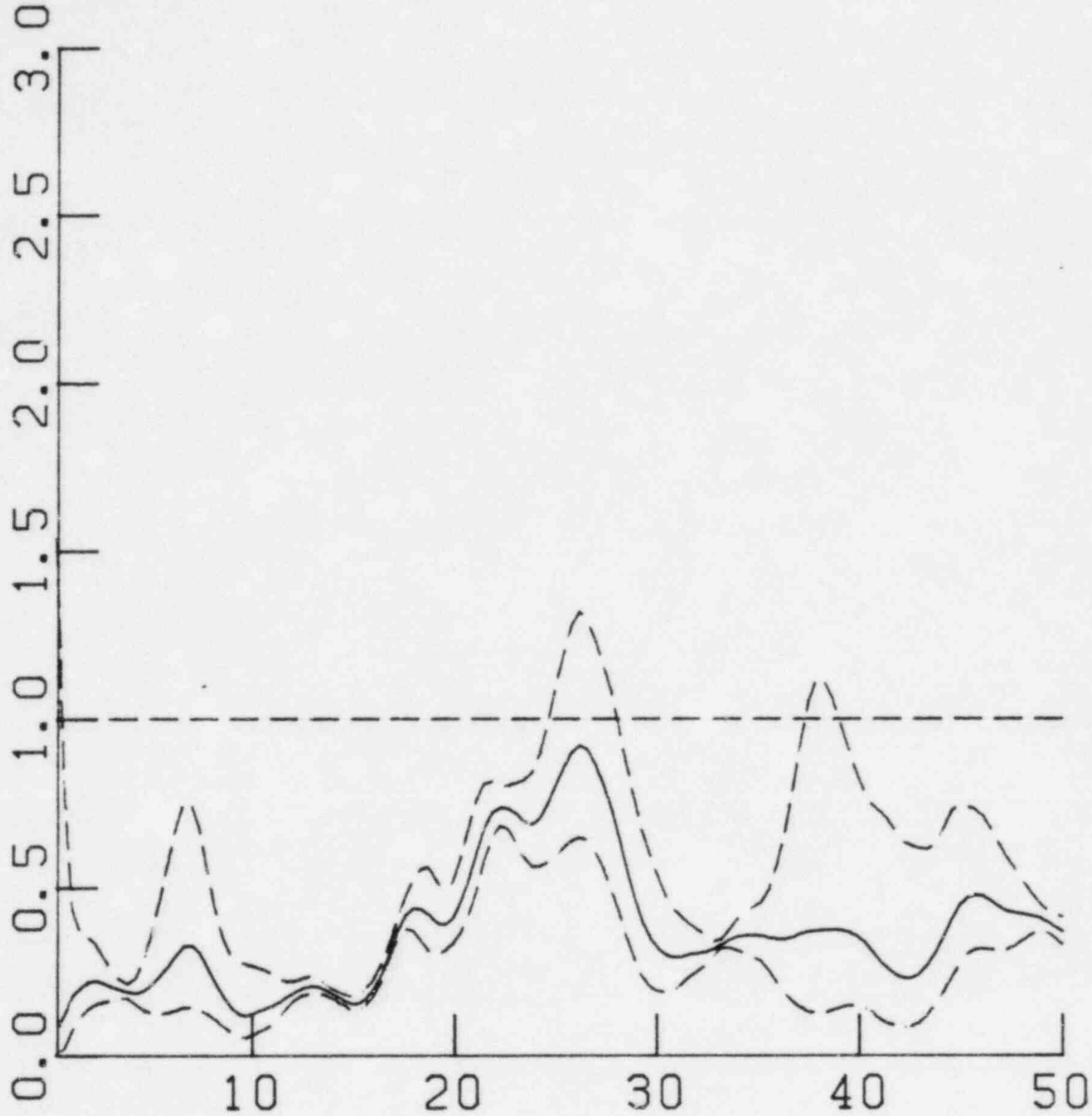

TEST 4 SHOTS:3 GS/<P3,F5> & 7,9 GS/F5 SRSS
RATIOS FROM MODULI INDIVIDUALLY
RUN NO 288
POWER SPECTRAL NOISE SUBTRACTED

Figure IX.C.5 Diesel Generator Building foundation/free field SRSS spectral modulus ratio for Test 4. Compare with results in Figure VI.C.32.

URS/Blume

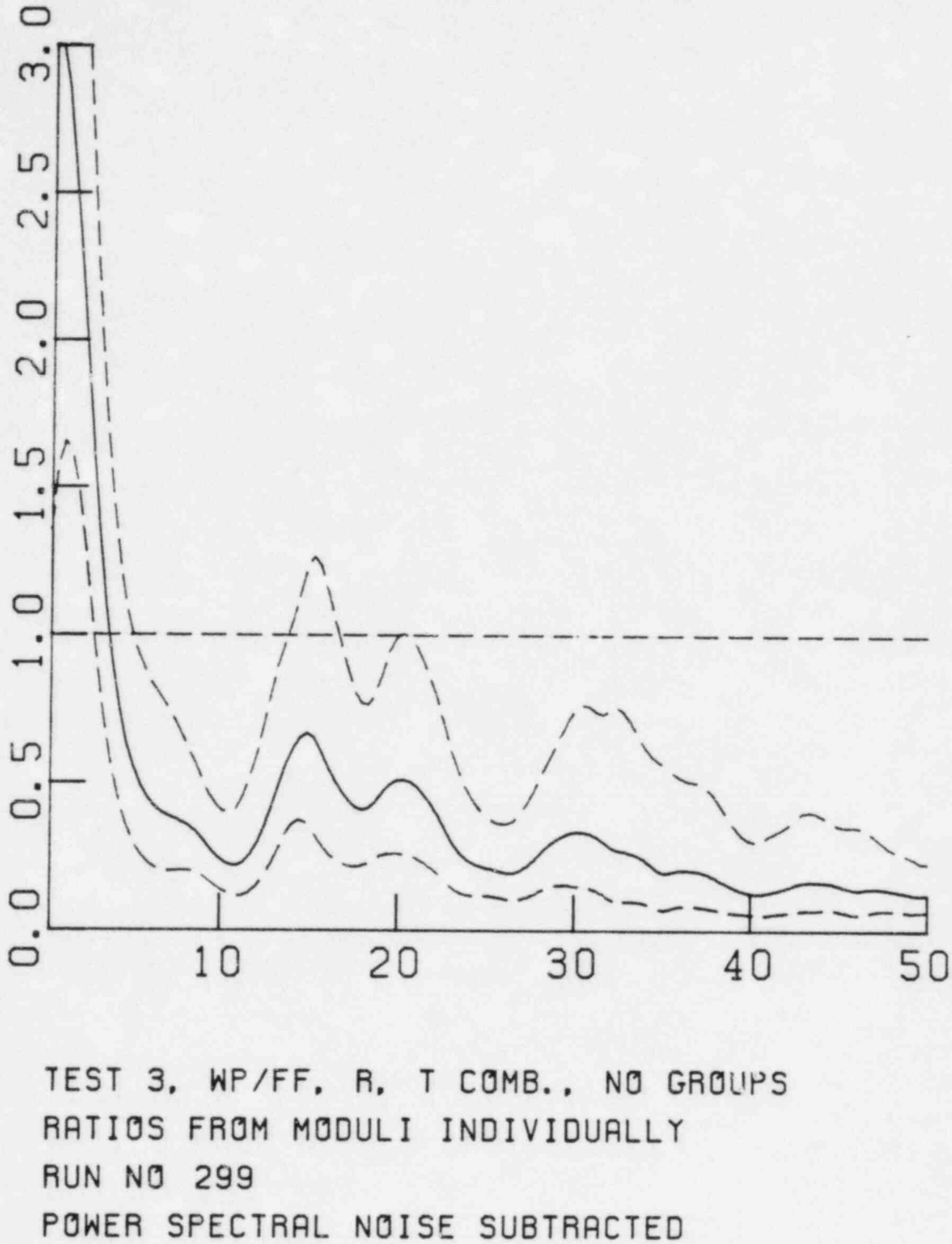

TEST 3, WP/FF, R, T COMB., NO GROUPS
RATIOS FROM MODULI INDIVIDUALLY
RUN NO 299
POWER SPECTRAL NOISE SUBTRACTED

Figure IX.D.1 Service Water Pumphouse foundation/free field spectral modulus ratio for combined horizontal components, with overall variability of the Test 3 data represented in the standard deviation bounds (dashed lines). Compare with Figures IX.C.1 and VI.C.16.

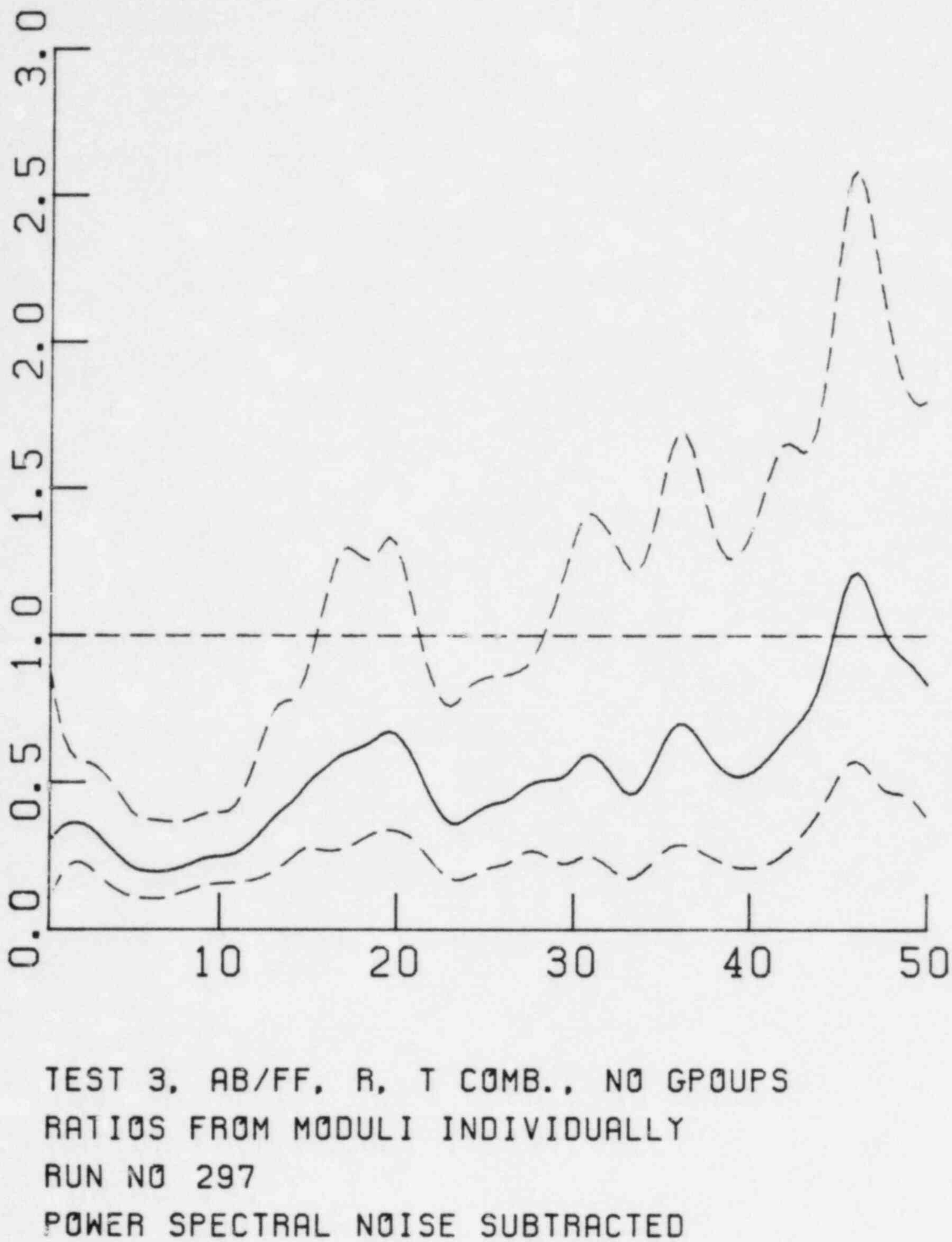

Figure IX.D.2 Auxiliary Building foundation/free field spectral modulus ratio for combined horizontal components, with overall variability of Test 3 data represented in the standard deviation bounds (dashed lines). Compare with Figures IX.C.2 and VI.C.20.

URS/Blume

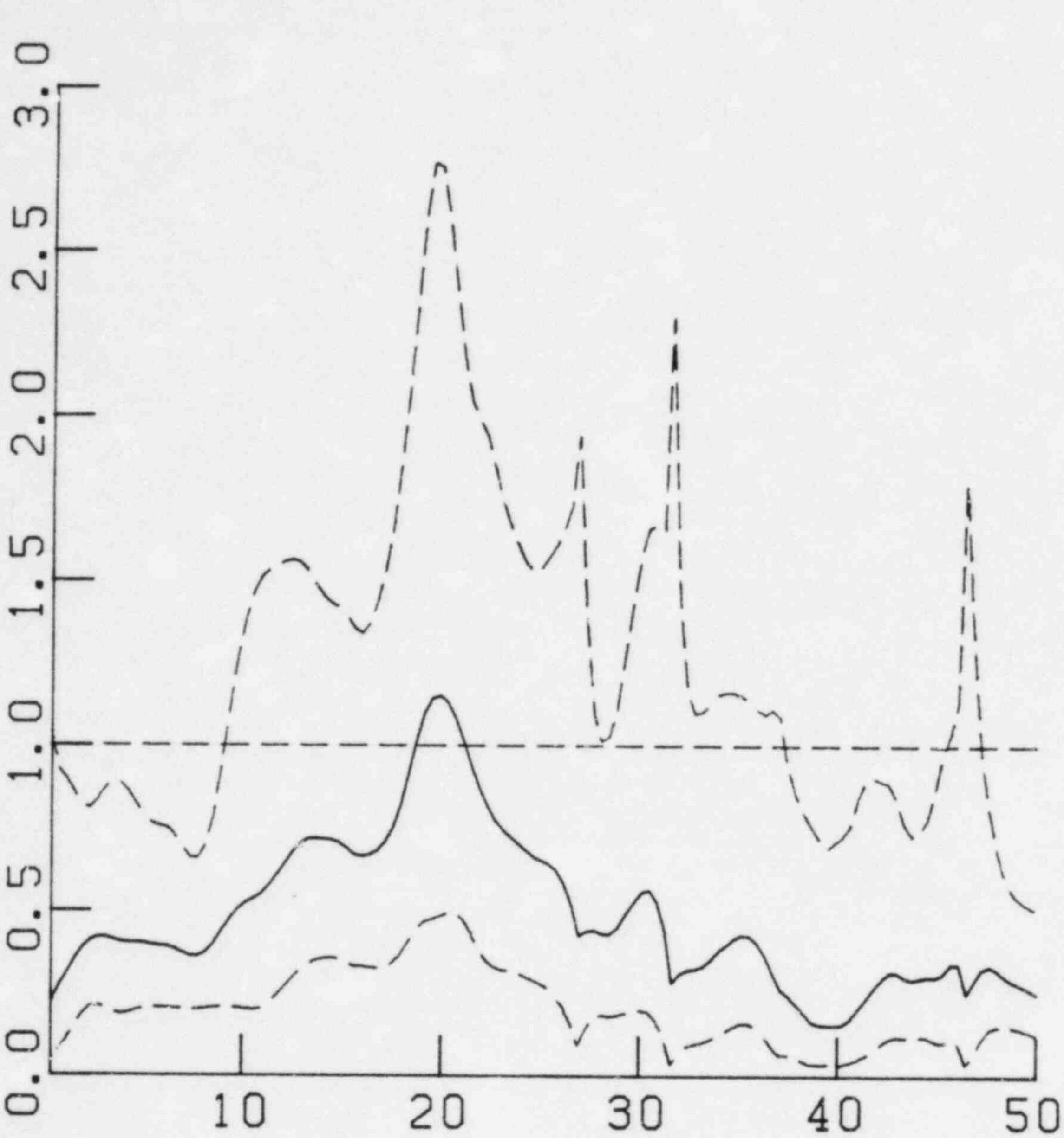

TEST 3, GS/FF, R, T COMB., NO GROUPS
RATIOS FROM MODULI INDIVIDUALLY
RUN NO 298
POWER SPECTRAL NOISE SUBTRACTED

Figure IX.D.3 Diesel Generator building foundation/free field spectral modulus ratio for combined horizontal components, with over all variability of Test 3 data represented in the standard deviation bounds (dashed lines). Compare with Figures IX.C.4 and VI.C.28.

URS/Blume